Integrated 3D Fibers/Hydrogel Biphasic Scaffolds for Periodontal Bone Tissue Engineering

Dario Puppi[1], Chiara Migone[1], Lucia Grassi[1], Alessandro Pirosa[1], Giuseppantonio Maisetta[2], Giovanna Batoni[2], Federica Chiellini[1]

[1]BIOLab Research Group, Department of Chemistry and Industrial Chemistry, University of Pisa, UdR INSTM Pisa, Pisa, Italy

[2]Department of Translational Research and New Technologies in Medicine and Surgery, University of Pisa, Pisa, Italy

*Corresponding author: Federica Chiellini, Department of Chemistry & Industrial Chemistry, University of Pisa, Via G. Moruzzi 13, 56124 Pisa (Italy); e-mail: federica.chiellini@unipi.it; Tel: +39-050-2219333

Keywords: tissue engineering, biphasic scaffold, poly(ε-caprolactone), chitosan, poly(γ-glutamic acid),

Abstract

Combining a tissue engineering scaffold made of a load-bearing polymer with a hydrogel represents a powerful approach to enhancing the functionalities of the resulting biphasic construct, such as its mechanical properties or ability to support cellular colonization. This research activity was aimed at the development of biphasic scaffolds through the combination of an additively manufactured poly(ε-caprolactone) (PCL) fibers construct and a chitosan/poly(γ-glutamic acid) polyelectrolyte complex hydrogel. By investigating a set of layered structures made of PCL or PCL/hydroxyapatite composite, biphasic scaffold prototypes with good integration of the two phases at the macro- and

microscale were developed. The biphasic constructs were able to absorb cell culture medium up to ten fold of their weight, and the combination of the two phases had significant influence on compressive mechanical properties compared with hydrogel or PCL scaffold alone. In addition, due to the presence of chitosan in the hydrogel phase, biphasic scaffolds exerted a broad-spectrum antibacterial activity. The developed biphasic systems appear well suited for application in periodontal bone regenerative approaches in which a biodegradable porous structure providing mechanical stability and a hydrogel phase functioning as absorbing depot of endogenous proteins are simultaneously required.

INTRODUCTION

Periodontal diseases are usually caused by pathogenic microbes forming a bio-film difficult to be eradicated, leading to inflammatory disorders, such as in the case of gingivitis and periodontitis[1, 2]. In addition, genetic and environmental factors as well as different diseases (e.g. dermatological and haematological) can contribute to periodontal disorders. In the case of periodontitis, the inflammation expands deep into the tooth-surrounding tissues and can result in loss of teeth, and degeneration of supporting connective tissue and alveolar bone[3]. While traditional periodontal treatments aim to remove the causes of the occurring infection, the ultimate goal of tissue engineering is regenerating the tissue defect[4]. Given the complex and hierarchically-structured nature of periodontal tissue, tissue engineering faces the repair of a variety of tissues including alveolar bone, periodontal ligament, cementum and gingival tissue[5]. A growing body of research has been focused on the development of periodontal polymeric scaffolds, such as injectable hydrogels or three-dimensional (3D) porous constructs[6]. As examples, calcium phosphate-coated melt electrospun poly(ε-caprolactone) (PCL) meshes were investigated as scaffolds for periodontal bone regeneration in combination with decellularized[7] or intact[8] periodontal ligament cell sheets to achieve periodontal attachment formation and cementum regeneration. Strategic biomimicry could be imparted through the use of multiphasic scaffolds designed for the functional integration of the different periodontal soft and hard tissue components with one another or with the host environment[9]. To this aim, various strategic scaffold multiphasic architectures have been developed: bone scaffolds combined with an occlusive membrane[10, 11], layered biphasic scaffolds for bone and ligament compartment[12-16], and layered triphasic scaffolds for cementum, periodontal ligament, and bone compartment[17].

Regenerative approaches toward *in situ* periodontal tissue regeneration are frequently based on endogenous resources, such as cells and growth factors[4]. The most exploited strategy involves a scaffolding material (e.g. fibrin, collagen and Emdogain® gel),in combination with autogenic growth factors, used to either recruit host stem cells or to inject encapsulated autogenic cells (e.g.

gingival stem cells[18] or fibroblasts[19]). A reliable alternative that has found clinical translation for periodontium regeneration treatments involves the functionalization of a scaffold with platelet rich plasma (PRP), an autologous platelets concentrate prepared from patient's own blood as a source of key endogenous growth factors and proteins. As recently reviewed[20, 21], a number of clinical trials have shown that PRP could be combined with different materials, such as bovine xenograft[22], bioactive glass[23], hydroxyapatyte[24] and β-tricalcium phosphate[25], to achieve enhanced healing of human intrabony defects. Platelet-rich fibrin (PRF) is a second generation platelet concentrate consisting of a strong natural fibrin matrix prepared from the patient's own blood by centrifugation without using any anticoagulant or other artificial biochemical modifications. This approach has found clinical application in periodontal tissue regeneration thanks to the possibility of obtaining directly from the blood a fibrin gel which concentrates almost all the platelets and growth factors of the blood specimen[26].

PCL is a biodegradable polyester widely investigated for biomedical applications because of its good biocompatibility, inexpensive production routes, tunable biodegradation kinetics and mechanical properties, and good blend-compatibility[27]. In addition, thanks to its good rheological and viscoelastic properties, PCL has been successfully processed into a wide range of porous scaffolds structured at the micro- and nano-scale[28]. For instance, PCL layered microfibrous structures[29] and nanofibrous assemblies[30] were recently investigated as bone tissue engineering scaffolds. However, PCL slow biodegradation (years for complete *in vivo* absorption[31]) could limit its application as biodegradable implant for periodontal applications. In fact, as pointed out by Rasperini *et al*.[16], a more rapidly resorbing scaffold would be better suited for the treatment of a periodontal osseous defect to avoid wound dehiscence and subsequent microbial contamination in a perimucosal environment around teeth. In addition, being hydrophobic in nature, polyesters like PCL cannot be directly functionalized with platelet concentrates to develop bioactive scaffolds for endogenous regenerative treatments. The strategy followed in this study to overcome such

drawbacks was to combine a low molecular weight PCL processed into a highly porous scaffold with a hydrogel phase with a faster degradation rate and swelling properties.

Hydrogels have attracted great interest as scaffolding material owing to their ability to absorb aqueous medium up to thousands of times their dry weight, to encapsulate cells and bioactive molecules as well as to allow efficient mass transfer[32]. In addition, hydrogels based on polymers from natural resources possess inherent biocompatibility, biodegradability and biologically recognizable moieties that could support cellular activities. Chitosan (CS)/poly(γ-glutamic acid) (γ-PGA)hydrogels represent a successful example of 3D swollen structures obtained through ionic complexation of two naturally-derived polymers[33, 34]. However, typical shortcomings of hydrogels limiting their application for biomedical purposes are their mechanical weakness and lack of mechanical integrity, poor control over pore size and difficulty to directly shape them in predesigned geometries by Additive Manufacturing (AM)[35].

This study aims to contribute to the growing area of periodontal bone tissue engineering research by exploring the development of biphasic scaffolds composed of a layered PCL porous construct obtained by computer-aided wet-spinning (CAWS) and a CS/γ-PGA polyelectrolyte complex (PEC) hydrogel. As recently reported[29], CAWS technique allowed to fabricate layer-by-layer PCL and PCL/hydroxyapatyte (HA) nanocomposite scaffolds with customized external shape and internal fully-interconnected porous architecture that well supported bone regeneration processes *in vitro*. Cell culture experiments employing the MC3T3-E1 preosteoblast cell line showed good cell adhesion, proliferation, alkaline phosphatase activity and bone mineralization on the developed PCL-based scaffolds[29]. CS/γ-PGA PEC hydrogels are characterized by high swelling degree and stability in aqueous solutions as well as the ability to support *in vitro* balb/3T3 mouse embryo fibroblasts adhesion and proliferation[33, 34]. Therefore, the specific objective of this study was to couple the mechanical strength, slow degradation and controlled porous microstructure of PCL-based scaffolds to the swelling properties of a CS/γ-PGA hydrogel exploitable for proteins absorption in regenerative medicine approaches. To this end, a novel experimental procedure for

combining the two phases by immersion of a PCL-based scaffold into a CS/γ-PGA mixture was explored. PCL and PCL/HA scaffolds with different pore size, and CS/γ-PGA mixtures with different composition were investigated to develop a set of biphasic polymeric constructs. Biphasic scaffold prototypes were characterized for their morphology by Scanning Electron Microscopy (SEM), thermal properties by Thermogravimetric Analysis (TGA) and Differential Scanning Calorimetry (DSC), swelling properties in PBS 1x at 37°C, and compressive mechanical properties by an uniaxial testing machine. In addition, the antibacterial activity of the biphasic constructs was tested against *Staphylococcus epidermidis* and *Escherichia coli*, selected as representative species of Gram-positive and Gram-negative bacteria, respectively.

EXPERIMENTAL

Materials

Poly(ε-caprolactone) (PCL, CAPA 6500, Mw = 50000 g/mol) was supplied by Perstorp Caprolactones Ltd (Warrington,UK). Chitosan (CS, medium molecular weight, Mw = 108 kDa, deacetylation degree ~ 92%) and hydroxyapatite nanoparticles (size < 200 nm) were bought from Sigma-Aldrich (Milan, Italy). Poly(γ-glutamic acid) (γ-PGA, 100 kDa) was obtained from Natto Bioscience (Osaka, Japan).

Preparation of PCL and PCL/HA scaffolds

PCL pellets were dissolved in acetone at 35 °C for 2 h under gentle stirring to obtain homogeneous solutions at the desired concentration (20% w/v). For the production of PCL/HA composite scaffolds, HA nanoparticles (1:4 HA/PCL weight ratio) were added to the polymeric solution and left under vigorous stirring at 35 °C for 1 h until a homogeneous dispersion of the nanoparticles was achieved. Scaffold manufacturing was performed by means of a computer-controlled rapid prototyping machine (MDX-40A, Roland DG Mid Europe Srl, Italy), modified in-house to allow the production of 3D scaffolds composed of wet-spun polymeric fibers[36]. The prepared solution was

placed into a plastic syringe fitted with a stainless steel blunt needle, i.d. 0.41 mm (gauge 22). A syringe pump (NE-1000, New Era Pump Systems, Wantagh, NY) was used to control the extrusion flow rate of the polymer solution into the coagulation bath. A beaker containing ethanol was fixed to the fabrication platform and used as coagulation bath. The 3D geometrical scaffold parameters, including the distance between the fiber axis (d_{xy}), layer thickness, scaffold external geometry and sizes, were designed using an algorithm developed in Matlab software (The Mathworks, Inc.). The combination of the X–Z axis needle motion and the Y axis platform motion allowed the fabrication of scaffolds layer-by-layer.The manufactured scaffolds were removed from the coagulation bath, kept under a fume hood overnight and then in a vacuum chamber for 48 h.

Preparation of Biphasic Scaffolds

CS/γ-PGA mixtures (80:20 weight ratio) were prepared by dissolving γ-PGA in dH_2O under stirring for 1 h at room temperature. The desired amount of CS was then added to the γ-PGA solution, and the suspension was left under vigorous stirring for 2 h. Acetic acid (1 % v/v) was finally added and the obtained mixture was left under overnight stirring. The total concentration of the polymeric phase in the mixture was either 5 or 2.5 % w/v. For the preparation of biphasic scaffolds, PCL and PCL/HA wet-spun samples were placed into a 12-well tissue culture plate, covered with a CS/γ-PGA solution (4 mL for each sample) and left 5 h at room temperature. The PCL-based scaffolds were periodically turned upside down to allow a good infiltration of the solution into the scaffold pores. The samples were then frozen at -20 °C for 24 hours, lyophilized for 72 hours (-50 °C, 0.04 Torr) and then stored in a desiccator.

Morphological Characterization

Morphology of the developed scaffolds was analyzed using Scanning Electron Microscopy (SEM) using a JEOL LSM 5600LV microscope (Tokyo, Japan) under backscattered electron imaging. Fiber diameter and pore size were measured by means of ImageJ 1.43u software (National Institutes

of Health, Bethesda, MD) on SEM micrographs with a 35x magnification. Data were calculated over 20 measurements per scaffold.

Determination of Swelling Degree

Swelling study of the prepared samples was carried out in Dulbecco's Modified Eagle Medium (DMEM) (Sigma Aldrich, Milan, Italy). At different time intervals, the samples were weighted after wiping out the surface swelling media with a filter paper. Experiments were performed in triplicate and the percentage swelling degree (SD) was calculated as:

$SD = [(W_s - W_d)/W_d] \times 100$

where W_d is the weight of the dry sample and W_s is the weight of the swollen sample.

Thermal Characterization

Thermogravimetric analysis (TGA) was performed using a TGA Q500 instrument (TA Instruments, Milan, Italy) under a constant nitrogen flow of 60 ml/min, in the temperature range 25-600 °C, and at a constant heating rate of 10 °C/min. The onset temperature (T_{onset}), given by the intersection of the tangent to the baseline with the tangent to the inflection point of the TGA curve, was considered as the starting degradation temperature. Differential Scanning Calorimetry (DSC) analysis was performed in the range -100 to 200 ºC at a heating rate of 10 ºC/min, cooling rate of 10 °C/min and under a nitrogen flow rate of 80 mL/min, using a Mettler DSC-822E instrument (Mettler Toledo, Milan, Italy). Glass transition temperature (T_g) was evaluated by analyzing the inflection point, while melting temperature (T_m) and percentage crystallinity (C%) by analyzing the endothermic peaks in the DSC heating scans. Three samples for each kind of scaffolds were tested in both thermal analyses.

Mechanical Characterization

Scaffolds compressive mechanical properties were analyzed using an uniaxial testing system (Instron 5564, Norwood, MA) with a 2 kN load cell. The test was conducted in air at room temperature after 8 h of submersion in PBS 1x. PCL and PCL/HA scaffolds with a square base area of 10 x 10 mm^2 and a thickness of around 5 mm (50 layers), and biphasic scaffolds with a

cylindrical geometry (diameter around 20 mm and thickness around 7 mm) were tested. Five samples of each kind of scaffold were characterized at a cross head speed of 1 mm/min between two parallel steel plates up to a maximum strain of 90%. The stress was defined as the measured force divided by the total area of the apparent cross-section of the scaffold, whilst the strain was evaluated as the ratio between the scaffold height variation and its initial height. Compressive modulus was calculated from the stress–strain curves as the slope of the initial linear region. Representative stress values taken at 50 and 90% of strain were reported in order to quantitatively support the graphical observation that PCL scaffolds were reinforced at high strain by the presence of an infiltrated hydrogel phase.

Antibacterial activity assay

The antibacterial activity of biphasic scaffolds was evaluated against *S. epidermidis* (ATCC 35984)as a model of Gram-positive bacteria and *E. coli*(ATCC 25922)as a model of Gram-negative bacteria. Bacterial cells were cultured in Mueller-Hinton Broth (Oxoid, Basingstoke, UK)for 18 h at 37°C,subsequentlydiluted in fresh medium and grown until exponential phase was reached. A volume of 200 µL of each bacterial suspension, containing approximately $2x10^6$ CFU (Colony Forming Units), was added to 20 mL of MHB in the presence of PCL (or PCL/HA) scaffold, biphasic scaffolds or CS/γ-PGA hydrogel. Bacteria suspended in MHB alone were used ascell growth control. Samples were incubated at 37°Cwith shaking for 6h (for *E. coli*) or 8 h (for *S. epidermidis*), regarding to the growth rate of each bacterial strain. At different times of incubation, the density of bacterial cultures was determined by measuring the optical density at 600 nm (OD_{600}) using a UV/Vis spectrophotometer (GeneQuant Pro, Pharmacia, Sweden).

Statistical Analysis

The data are represented as mean ± standard deviation. Statistical differences were analyzed using one-way analysis of variance (ANOVA), and a Tukey test was used for post hoc analysis. A p value < 0.05 was considered statistically significant.

RESULTS AND DISCUSSION

Biphasic Scaffolds Development

An experimental procedure for the preparation of biphasic constructs composed by an additively manufactured 3D PCL-based porous structure and a hydrogel phase made of a CS/γ-PGA PEC was developed. On the basis of a previous study regarding the development of a CAWS technique for the layered manufacturing of scaffolds made of PCL (Mw = 80000)[29], the processing conditions for the obtainment of 3D structures made of a PCL with a lower Mw (50000 g/mol) were investigated. The manufacturing process involved the continuous extrusion of a polymeric solution through a needle immersed into an ethanol coagulation bath.3D scaffold architectures were built up with a layer-by-layer process by depositing the solidifying filament with a 0–90° lay-down pattern(Fig. 1a).The optimized PCL scaffolds fabrication parameters were: polymer concentration = 20 % w/v, initial needle tip-collection platform distance = 2 mm, deposition velocity = 240 mm/min, solution feed rate = 1 mL/h and inter-layer needle translation = 0.1 mm. By applying these parameters, prototypal PCL scaffolds with different pore size were developed by changing the inter-fiber needle translation distance (d_{xy}) in the range 0.5 to 2 mm (Figure 1b).

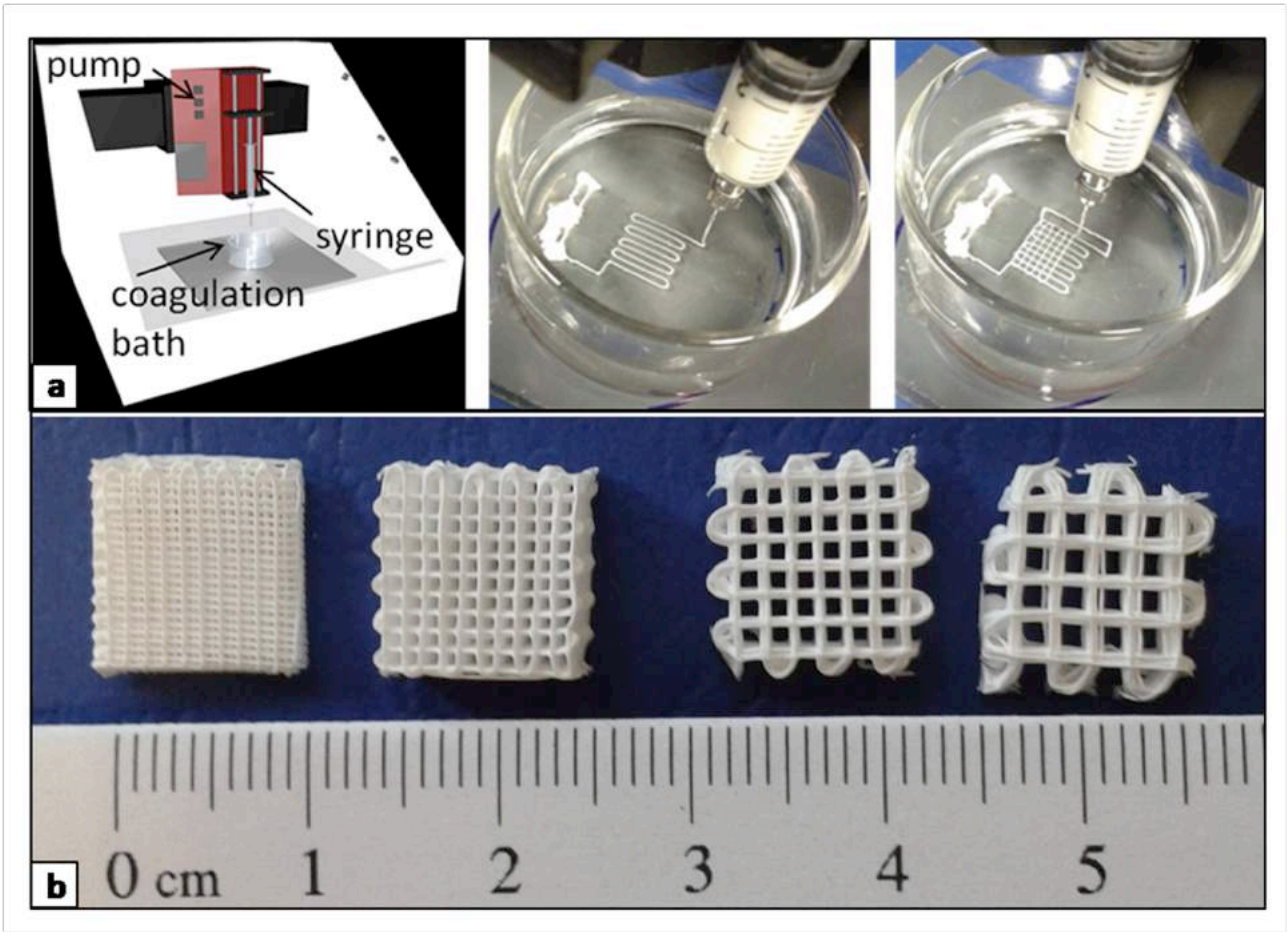

Figure 1. PCL scaffolds fabrication by computer-aided wet-spinning (CAWS): (a) schematics of CAWS apparatus and layer-by-layer production process; (b) PCL scaffolds (10x10 mm, 50 layers) with different pore size due to variation in inter-fiber needle translation (from left to right d_{xy}= 0.5, 1, 1.5 and 2 mm).

HA-loaded PCL scaffolds with the same structural characteristics were manufactured by applying the optimized processing parameters to polymeric solutions containing the inorganic particles as suspension (Figure 2a). Biphasic constructs were developed by immersing PCL-based scaffolds in a CS/γ-PGA solution and followed by freeze-drying. As shown in figure 2b, a relatively too high CS/γ-PGA solution concentration did not allow to achieve the required integration between the two phases. However, by decreasing CS/γ-PGA concentration to 2.5% w/v, the hydrogel phase fully penetrated into the PCL porous architecture leading to the formation of an integrated biphasic structure (Figure 2c). By employing this concentration, four biphasic construct prototypes based on either PCL or PCL/HA scaffolds in combination with a CS/γ-PGA hydrogel were developed (Fig.

2d). In the dry state the hydrogel portion of the biphasic scaffolds resulted physically spongy and could be easily handled without breaking. Scaffolds obtained applying d_{xy}= 0.5 mm ($PCL_{0.5mm}$ and $PCL/HA_{0.5mm}$) were excluded from the study since the small pore size did not allow good hydrogel penetration even in the case of low solution concentration. In addition, PCL scaffolds with d_{xy}= 2 mm (PCL_{2mm} and PCL/HA_{2mm}) were not further investigated because of the flattened fiber morphology at the crossing points leading to the collapse of the 3D structure along Z axis.

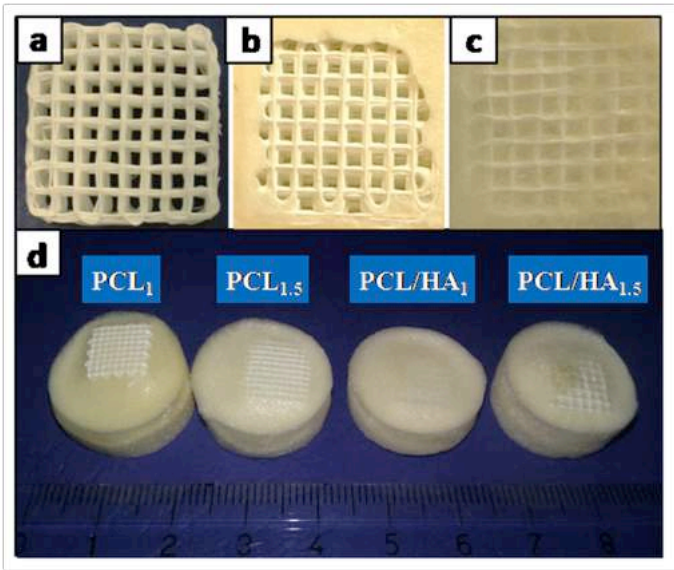

Figure 2. Development of biphasic constructs. Representative photographs of (a) a PCL/HA_1 scaffold, (b) biphasic construct obtained employing a PCL/HA_1 scaffold and a 5 % w/v CS/γ-PGA solution, (c) biphasic construct obtained employing a PCL/HA_{1mm} scaffold and a 2.5 % w/v CS/γ-PGA solution; (d) four biphasic construct prototypes based on PCL or PCL/HA scaffolds in combination with a CS/γ-PGA 2.5 % w/v solution (Measure unit = 1 mm).

The combination of a fibrous polymeric network and a hydrogel phase can represent a powerful tool for the optimization of overall scaffold functionalities, such as mechanical properties, cellular colonization and swelling properties. It can be also seen as a biomimetic approach aimed at the obtainment of a complex composite reproducing the fibrous protein framework supporting the aqueous component in different native tissues[37]. Hydrogels have been combined with a wide array of fibrous structures, such as carbon nanotubes[38, 39], polymeric nano-[40] and microfibers[41], polymeric

wovens[42, 43] and non-wovens[44], and polymeric layered scaffolds by AM[37, 45-50]. For instance, Liao *et al*.[43] developed a potential acellular or cell-based scaffold with tunable mechanical and tribological properties mimicking those of native cartilage, by infiltrating a woven PCL fiber construct with an interpenetrating dual-network "tough-gel" consisting of alginate and polyacrylamide. In another study Yu *et al*.[45] demonstrated that cellular-loading efficiency and cells colonization of layered PCL scaffolds could be enhanced through combination with a stem cell-seeded collagen hydrogel. The present study makes a noteworthy contribution to this research trend by providing a novel biphasic structure combining layered PCL scaffolds with a PEC hydrogel that could function as potential depot for endogenous proteins in regenerative approaches. In addition, an integrated hydrogel phase infiltrated into the porous scaffold network enables to employ larger scaffold pores size without potentially compromising the cellular colonization of inter-fiber gaps. Such a system would have a faster degradation due to the lower PCL ratio in the biphasic construct. This aspect, together with the employment of a relatively low polymer molecular weight (50000 g/mol), can allow increasing the scaffold degradation rate.

Morphological Analysis

SEM image analysis was carried out to assess the integration between the PCL scaffold and the PEC hydrogel at the macro- and microscale. The morphological investigation highlighted that PCL scaffolds were characterized by a spongy morphology of the deposited fiber constituting the 3D layered structure (Figure 3a).

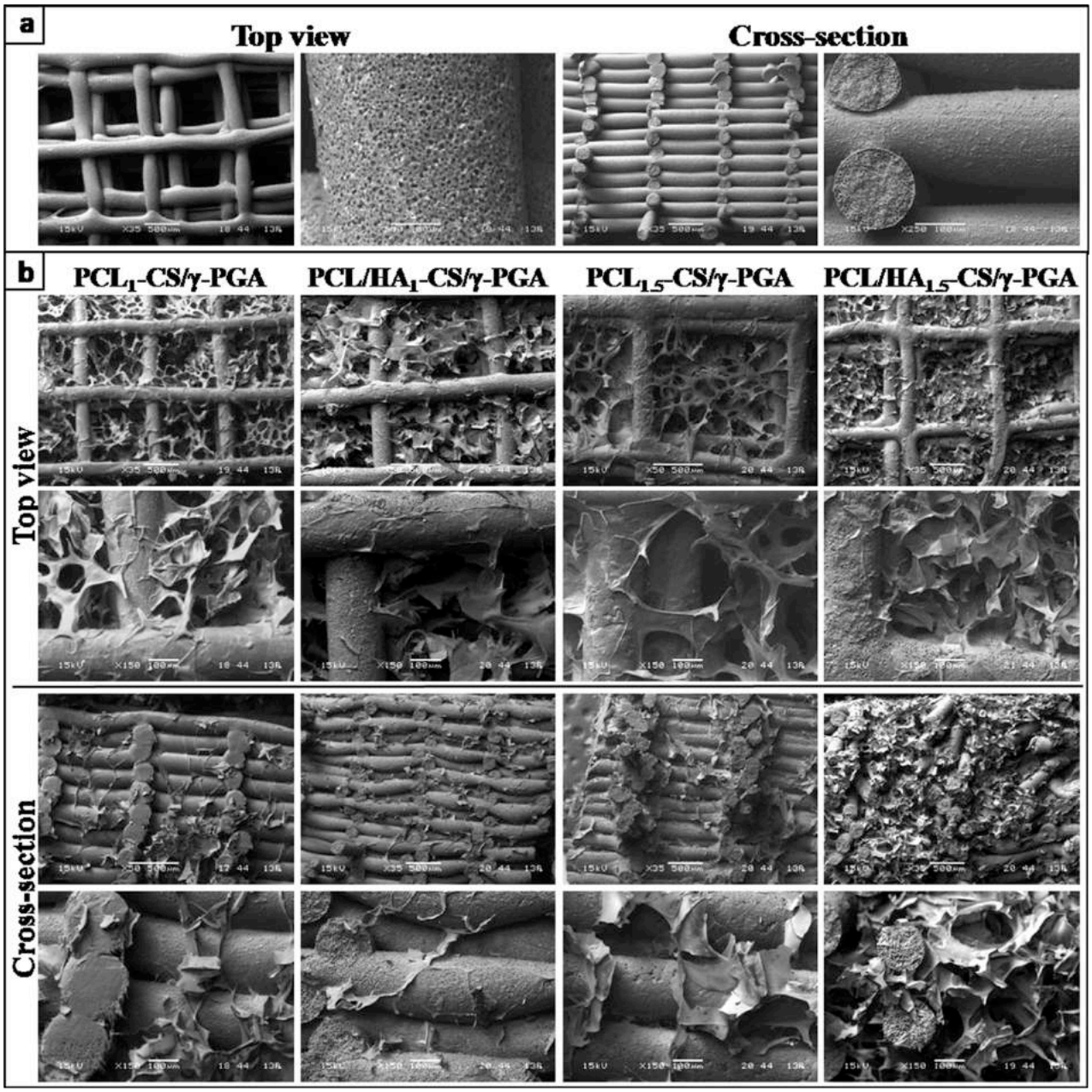

Figure 3. Morphological analysis by Scanning Electron Microscopy (SEM).Representative backscatter SEM micrographs taken at different magnifications from the top view and cross-section of (a) PCL_1 scaffolds and (b) biphasic construct prototypes.

As widely discussed in previous published papers[29, 36], such microporosity is to be ascribed to the phase inversion process governing polymer solidification. In fact, the solvent/non-solvent exchange during polymer solidification leads to the formation of a polymer-rich phase and a polymer-lean phase that will finally result in pores formation in the fiber polymeric matrix. Differently from what commonly obtained by means of melt-extrusion-based AM techniques, CAWS approach allows to

develop hybrid architectures with both globally and locally porosity[51]. The resulting fiber microporosity can be tuned in a certain range by acting on different phase inversion parameters (e.g. polymer concentration and deposition velocity). This can allow to tailor scaffold biodegradation rate, mass transfer phenomena associated to cell activities and release of loaded drugs, as well as the surface roughness influencing cell adhesion and proliferation[52].

Dimensional analysis of the scaffolds structural parameters revealed a fiber diameter in the range 200-300 μm and a XY pore dimension that varied from 200 to 1800 μm by increasing d_{xy} from 0.5 to 2.0 μm(Table 1). The presence of HA nanoparticles in the polymeric matrix did not remarkably influence the two investigated structural parameters. Fiber diameter was not significantly affected by d_{xy} variation, except in the case of PCL scaffolds obtained with d_{xy} = 2 mm characterized by a larger fiber size. This is likely due to fiber flattening at crossing points, strictly related to the lower layer fabrication time.

SEM analysis corroborated macroscopic observations in highlighting the good integration between the PCL porous scaffold and the hydrogel phase in all the developed biphasic constructs (Figure 3b). The hydrogel phase uniformly infiltrated into the inter-fiber pores and was also clearly visible in the whole scaffold cross-section. As shown in high magnification micrographs, the hydrogel well adhered to the PCL fibers forming a cohesive biphasic interface. In addition, from top view micrographs it is particularly evident the porous structure of the hydrogel phase that could be favorable to cell penetration and proliferation[53].

Different strategies have been explored to develop biphasic scaffolds constituted by a layered load-bearing structure by AM integrated with a hydrogel phase. For instance, Bioprinting techniques were applied to manufacture cell-laden constructs by simultaneously[46] or alternatively[47, 48] depositing extruded PCL melt and hydrogel. In this case, PCL and hydrogel strands were either combined in each layer or alternatively organized in successive layers. Other articles reported on a procedure similar to that adopted in the current study, involving the soaking of a scaffold into a mold containing a pre-gel solution or the dropping of the hydrogel-forming mixture onto the

scaffold[37, 49, 50]. Although these studies demonstrated the structural reinforcement of the investigated hydrogel by combination with a 3D fibrous structure, they lack of a micro-morphological analysis of the construct cross-section as well as the fiber/hydrogel interface. As demonstrated in this study, parameters like hydrogel solution viscosity and fiber scaffold pore size determine the integration of the hydrogel in the porous constructs. In addition, other factors such as electrostatic interactions, polymers hydrophilicity/hydrophobicity and fiber surface roughness, influence the adhesion of the hydrogel to the fiber surface. The SEM characterization reported in this research will serve as a basis for future studies on analogous biphasic scaffolds involving a detailed investigation of the actual integration at the macro- and microscale between the employed hydrogel phase and the fiber network.

Thermal Analysis

The thermal properties of the developed scaffolds were investigated to assess the effect of material processing, HA loading and biphasic structure preparation on the PCL macromolecular structure parameters obtainable from TGA and DSC analysis. Representative thermograms of the investigated samples are shown in Figure 4, while the obtained thermal parameters are reported in Table 2 .

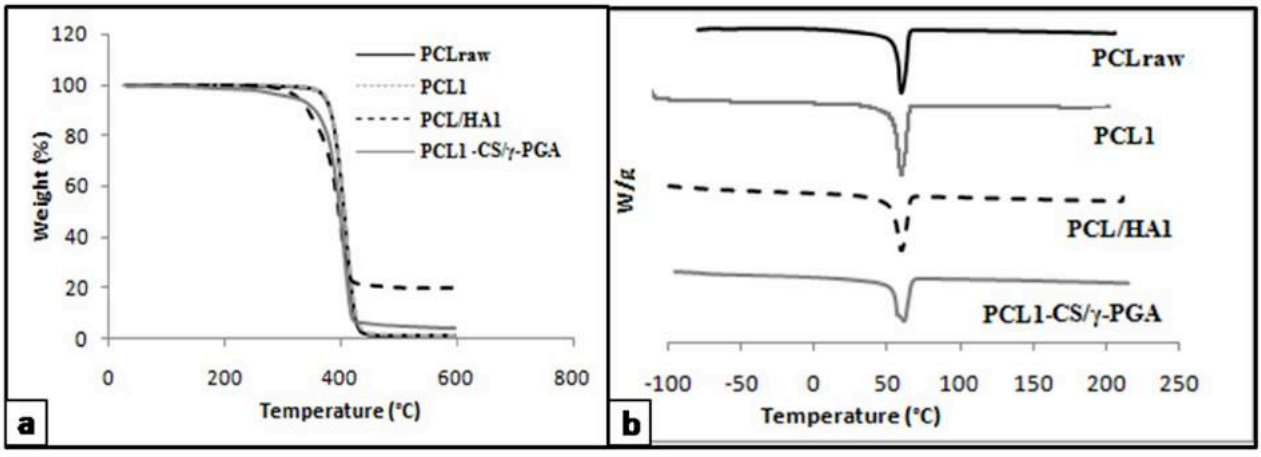

Figure 4. Thermal properties assessment. Representative TGA (a) and first heating DSC (b) thermograms of raw PCL, PCL_1, PCL/HA_1 and PCL-CS/γ-PGA scaffolds.

PCL scaffolds were characterized by a thermal degradation profile overlapping with that of unprocessed PCL (T_{onset} around 385 °C) in agreement with other studies suggesting that CAWS processing does not alter the polymer molecular structure[36, 54]. HA-loaded scaffolds had a lower thermal stability (T_{onset} = 347.26 ± 11.18 °C) than plain scaffolds as well as raw polymer, supporting results from previous research on the development of PCL/HA composite scaffolds[55]. The weight residue at 600 °C for PCL/HA_1 scaffolds was 22.20 ± 2.02%. This value can be related to the actual content of the ceramic in the composite and roughly corresponded to the percentage weight of HA added to the polymer solution. CS/γ-PGA PEC hydrogels (T_{onset}= 293.01 ± 11.95 °C) showed faster weight loss in comparison to the two constituting raw polymers ($T_{onset}$of 306.04 ± 2.08 °C for CS and 359.58 ± 1.38 °C for γ-PGA). This could be mainly related to the evaporation of residual water molecules physically/chemically-bound to the polymers as well to a reduced hydrogen bonding density in the CS structure due to the electrostatic interaction with γ-PGA[56-58]. Biphasic constructs (T_{onset} in the range 360-380 °C) exhibited significantly lower thermal stability compared to PCL_1 scaffolds due to the presence of the hydrogel phase.

DSC analysis showed that all the analyzed samples were characterized by an endothermic peak at around 60 °C ascribable to melting of PCL crystalline domains (Figure 4b). The comparative analysis of data from the first scan (Table 2) showed that wet-spun scaffolds had significantly higher T_m and crystallinity than raw polymer. This result is consistent with those of recent studies showing that in the wet-spinning process the non solvent-induced coagulation generally leads to high levels of polymer crystallinity[36, 54]. No statistically significant differences were observed when comparing data sets from second heating scan of raw PCL, PCL_1scaffolds and PCL/HA_1 scaffolds, in agreement with what found during TGA analysis, suggesting that the employed materials processing technique did not cause remarkable chemical-physical changes in polymer structure. T_m and crystallinity obtained from the endothermic peaks of biphasic scaffolds traces are statistically

comparable to those of PCL_1 scaffolds. It can therefore be assumed that the experimental procedure for biphasic scaffolds preparation did not alter the macromolecular architecture of wet-spun PCL.

Determination of the Swelling Degree

The swelling properties of the optimized biphasic scaffolds were studied in DMEM at 37°C (Figure 5a). As expected in virtue of the hydrophobic nature of PCL, the swelling degree (SD) of PCL scaffolds, investigated at different time intervals up to ten hours of soaking, gave no appreciable SD values and thus it was not included in the graphic representation of the samples swelling behavior. All the analyzed samples showed similar SD curves characterized by a maximum value after 30 min of immersion reaching the equilibrium within few hours (Figure 5a). Scaffolds produced by employing a d_{xy} of 1.5 mm, were characterized by a significantly higher SD in the first hours, likely due to the larger pore size as well as lower PCL ratio in the biphasic construct. No significant differences were recorded between HA-loaded and unloaded biphasic scaffolds. The observed decrease of the SD within the first hour of soaking could be attributed to a partial loss of the polyanion component that is not involved in the formation of the PEC hydrogel. However, the good stability of the hydrogel phase penetrating the PCL fibrous structure is supported by the observed constant weight of the samples up to ten hours.

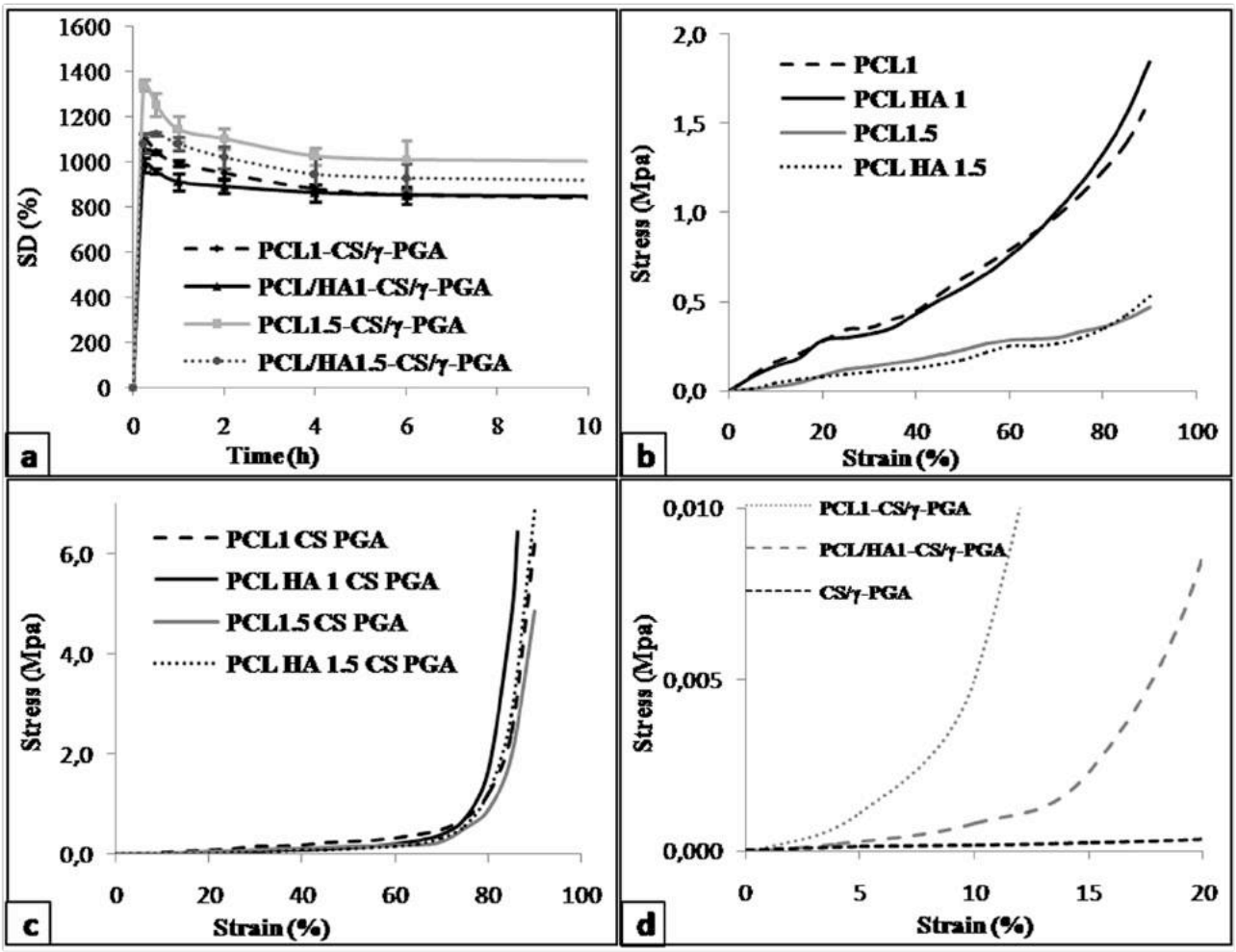

Figure 5. Swelling and mechanical behavior evaluation of the developed scaffolds:(a) Swelling degree (SD) curves of the optimized biphasic constructs in DMEM at 37°C.Representative compressive stress-strain curves of the developed scaffolds: (b) PCL based samples; (c) biphasic constructs; (d) biphasic constructs vs CS/γ-PGA hydrogel (strain rate = 1 mm/min and maximum strain = 90%; PBS 1x at 37°C).

Equilibrium swelling of PEC hydrogels is determined by the balance between the elastic retractile response of the polymeric network and the net osmotic pressure within the network due to the mobile counterions around the fixed charge groups[59]. At the equilibrium swollen state, the biphasic constructs increased their weight up to ten fold due to culture medium absorption by the hydrogel phase. The observed swelling values are comparable to those reported for porous CS/γ-PGA PEC hydrogels obtained by different techniques, such as freeze dryingand CAWS[33, 34], suggesting that the presence of the PCL layered structure doesn't remarkably affect the ability of the construct to

absorb an aqueous medium. This swelling ability could be exploited in tissue engineering strategies requiring scaffold absorption of great amounts of physiological fluids.

Mechanical Properties

The compressive mechanical properties of the developed scaffolds were evaluated using an unconfined uniaxial testing machine. Representative stress-strain curves of PCL and PCL/HA scaffolds are reported in Figure 5b.Scaffolds produced employing d_{xy} = 1 mm had significantly higher compressive modulus and strength than scaffolds produced employing d_{xy} = 1.5 mm because of the higher fiber packing density (Table 3).Although previous studies have shown that HA inclusion into a polymeric matrix fiber scaffold can lead to enhanced mechanical properties [29, 36, 60], an univocal effect of HA-loading on the compressive parameters of the developed scaffolds was not observed. As examples, while in the case of $PCL_{1.5}$ scaffolds an increased modulus upon HA loading was observed, in the case of PCL_1 scaffolds significantly lower modulus and strength was measured for loaded scaffolds.

All the tested biphasic scaffolds showed a similar compressive behavior characterized by a slow increase of the stress up to around a 60% strain, followed by a region with a fast increasing of the curve slope (Figure 5c). In comparison to PCL scaffolds, the biphasic constructs showed a lower compressive strength up to around 80% strain and a much higher strength in the subsequent region. In addition, the biphasic scaffolds displayed a stiffness 10 to 100 folds that of the CS/γ-PGA hydrogels (Figure5d, Table 3).

Most of the studies aimed at the mechanical reinforcement of hydrogels with a fibrous polymeric network reported on the employment of electrospun nonwovens with a resulting increase of stiffness one- to threefold in comparison to the hydrogel phase[61, 62].Visser *et al.*[37]developed a mathematical model to study the mechanical behavior of a gelatin methacrylate with increased stiffness through the combination with a highly aligned ultrafine PCL fiber architecture obtained by melt-electrospinning writing. They demonstrated that under axial compression the hydrogel phase places the PCL fibers under tension with the overall result of increasing the stiffness up to fiftyfold.

Since the incompressible nature of swollen polymers, each volume of the hydrogel phase confined into a scaffold cell expands in response to the applied stress causing fibers deformation. However, in the case of thicker fibers (> 88 μm)a mechanical reinforcement of the hydrogel was not achieved due to the stronger vertical column of fiber crossings causing water flowing out of the scaffold. Although the fiber size of the biphasic scaffolds reported in the present study is even larger (> 200 μm), it is likely that the higher flexibility of microporous wet-spun fibers in comparison to dense fibers by melt processing[29] allowed achieving a uniform deformation of PCL with enhancement of biphasic constructs compressive strength.

Antimicrobial Properties

The antibacterial activity of biphasic scaffolds against *S. epidermidis* ATCC 35984 and *E. coli* ATCC 25922 was evaluated by monitoring the bacterial growth in liquid cultures. As shown in figure 6, biphasic constructs were able to markedly inhibit the growth of both bacterial species. In particular, a15-fold decrease in the OD_{600} value compared to the untreated control was observed for *S. epidermidis* after 8 h of incubation (Fig. 6 a-b), while an approximately 4-fold reduction of optical density was assessed for *E. coli* after 6 h of incubation (Fig. 6 c-d). Hence, the antibacterial effect of biphasic scaffolds was compared with that of the PCL-based scaffolds and of the CS/γ-PGA hydrogel. For all time points tested, biphasic constructs caused a statistically significant reduction in the OD_{600}value compared to the PCL (and PCL/HA) scaffold, while no difference was observed as compared to the CS/γ-PGA hydrogel.

The results suggested that the antimicrobial properties of the whole system are due to the presence of CS. The antimicrobial activity of CS against many Gram-positive and Gram-negative bacteria has been well documented in the literature[63, 64]. Due to this bioactive property, CS has been previously investigated as scaffolding material in the clinical treatment of chronic periodontitis [65]. Although its exact mechanism of action is still unclear, it is likely that the polycationic structure of CS may interact electrostatically with the anionic components of bacterial surface (e.g. lypopolysaccharide and peptidoglycan) and target the cell membrane, leading to cell damage or

death[55]. A scaffold endowed with antimicrobial properties could be generally desired in order to respond to the elevated risk of infections from bacteria introduced during the surgical implantation [66]. In addition, the hours following an implantation procedure are crucial for the evolution of microbial infections, because the immune response is not active yet. A successful integration of the implanted scaffold with the host tissues is achieved only if a critical bacteria colonization of its surface is avoided. This becomes extremely challenging in the case of infectious-related periodontal diseases caused by bacterial species able to form a biofilm resistant to antibiotics[65]. In this context, the use of CS in the hydrogel phase could be a very promising approach to inhibit the short-term bacterial colonization of the scaffold thus favoring its integration into the periodontal defect site.

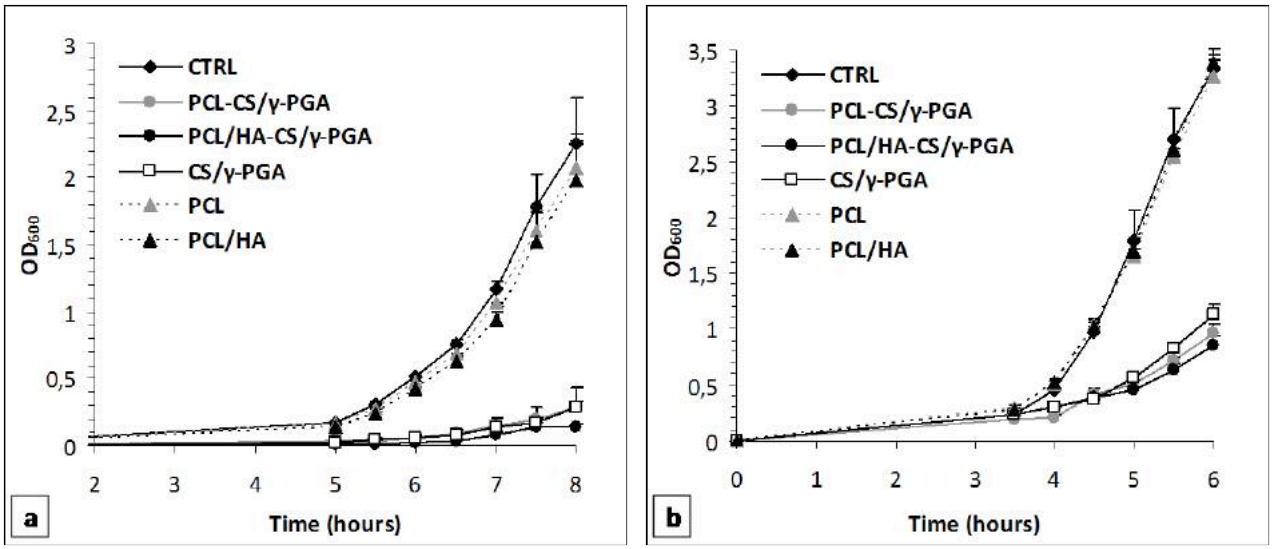

Figure 6. Antibacterial activity evaluation. Growth curves of *S. epidermidis* ATCC 35984 (a) and *E. coli* ATCC 25922 (b) in the presence of PCL-based scaffolds, biphasic constructs and CS/γ-PGA hydrogel. Controls (CTRL) represent untreated bacteria. Data are expressed as mean ± standard error of three independent experiments.

CONCLUSIONS

Combining a 3D PCL scaffold with a predefined porous architecture and good structural stability with a CS/γ-PGA PEC with good swelling properties could represent a synergistic tool for the development of biphasic scaffolds suitable to be functionalized by platelet concentrate absorption. The developed experimental method is well suited for the production of PCL-CS/γ-PGA biphasic

structures showing good integration at the macro- and microscale. As demonstrated by the comparative mechanical characterization, the biphasic structures were characterized by enhanced mechanical properties in comparison with the hydrogel alone. This result was not previously observed in studies on additively manufactured PCL scaffolds with relatively large fiber size, and could be attributed to the higher flexibility of wet-spun structures in comparison to melt-extruded structures as consequence of the fiber spongy morphology. Furthermore, the presence of CS confers antibacterial properties to the biphasic scaffolds, representing a useful tool to minimize the risk of bacterial proliferation at the site of implants and prevent implant failure.

The present study opens new possibilities for the development of innovative strategies focused on periodontal bone regeneration through the employment of bioactive scaffolds functionalized with autologous platelet concentrates. Future studies will address the ability of the developed biphasic constructs to absorb platelet concentrates and to support cellular colonization *in vitro*. The possibility of obtaining anatomically-shaped scaffolds by means of the developed preparation process is part of an ongoing research.

ACKNOWLEDGMENTS

This study was supported by a Tuscany Region (Italy) funded Project "Nuovi Supporti Bioattivi a Matrice Polimerica per la Rigenerazone Ossea in Applicazioni Odontoiatriche (R.E.O.S.S.)" as part of the program POR CReO FESR 2007-2013 - Le ali alle tue idee. Authors are grateful to Dr.Randa Ishak for her precious support in recording SEM images.

REFERENCES

1. Pihlstrom BL, Michalowicz BS and Johnson NW, *Lancet* **366**: 1809-1820 (2005).
2. Ford PJ, Gamonal J and Seymour GJ, *Periodontol 2000* **53**: 111-123 (2010).
3. Chen F-M and Shi S, Periodontal Tissue Engineering, in *Principles of Tissue Engineering (Fourth Edition)*, ed by Vacanti R, Lanza R and Langer J. Academic Press, Boston, pp. 1507-1540 (2014).
4. Abou Neel EA, Chrzanowski W, Salih VM, Kim H-W and Knowles JC, *J Dent* **42**: 915-928 (2014).
5. Rios HF, Lin Z, Oh B, Park CH and Giannobile WV, *J Periodontol* **82**: 1223-1237 (2011).

6. Ramseier CA, Rasperini G, Batia S and Giannobile WV, *Periodontol 2000* **59**: 185-202 (2012).
7. Farag A, Vaquette C, Theodoropoulos C, Hamlet SM, Hutmacher DW and Ivanovski S, *Journal of Dental Research* **93**: 1313-1319 (2014).
8. Dan H, Vaquette C, Fisher AG, Hamlet SM, Xiao Y, Hutmacher DW and Ivanovski S, *Biomaterials* **35**: 113-122 (2014).
9. Ivanovski S, Vaquette C, Gronthos S, Hutmacher DW and Bartold PM, *Journal of Dental Research* **93**: 1212-1221 (2014).
10. Requicha JF, Viegas CA, Hede S, Leonor IB, Reis RL and Gomes ME, *J Tissue Eng Regener Med*: doi: 10.1002/term.1816. (2013).
11. Requicha JF, Viegas CA, Muñoz F, Azevedo JM, Leonor IB, Reis RL and Gomes ME, *Tissue Eng, Part A* **20**: 2483-2492 (2014).
12. Costa PF, Vaquette C, Zhang Q, Reis RL, Ivanovski S and Hutmacher DW, *J Clin Periodontol* **41**: 283-294 (2014).
13. Park CH, Rios HF, Jin Q, Bland ME, Flanagan CL, Hollister SJ and Giannobile WV, *Biomaterials* **31**: 5945-5952 (2010).
14. Park CH, Rios HF, Jin Q, Sugai JV, Padial-Molina M, Taut AD, Flanagan CL, Hollister SJ and Giannobile WV, *Biomaterials* **33**: 137-145 (2012).
15. Vaquette C, Fan W, Xiao Y, Hamlet S, Hutmacher DW and Ivanovski S, *Biomaterials* **33**: 5560-5573 (2012).
16. Rasperini G, Pilipchuk SP, Flanagan CL, Park CH, Pagni G, Hollister SJ and Giannobile WV, *Journal of Dental Research* **94**: 153S-157S (2015).
17. Lee CH, Hajibandeh J, Suzuki T, Fan A, Shang P and Mao JJ, *Tissue Engineering Part A* **20**: 1342-1351 (2014).
18. Fawzy E-S, Paris S, Becker S, Neuschl M and De Buhr W, *J Clin Periodontol* **39**: 861-870 (2012).
19. McGuire MK and Scheyer ET, *J Periodontol* **78**: 4-17 (2007).
20. Pandit N, Malik R and Philips D, *J Indian Soc Periodontol* **15**: 328-337 (2011).
21. Sell SA, Ericksen JJ and Bowlin GL, *Polym Int* **61**: 1703-1709 (2012).
22. Hanna R, Trejo PM and Weltman RL, *J Periodontol* **75**: 1668-1677 (2004).
23. Demir B, Şengün D and Berberoğlu A, *J Clin Periodontol* **34**: 709-715 (2007).
24. Yamamiya K, Okuda K, Kawase T, Hata K-i, Wolff LF and Yoshie H, *J Periodontol* **79**: 811-818 (2008).
25. Döri F, Huszár T, Nikolidakis D, Tihanyi D, Horváth A, Arweiler NB, Gera I and Sculean A, *J Periodontol* **79**: 660-669 (2008).
26. Preeja C and Arun S, *Saudi J Dent Res* **5**: 117-122 (2014).
27. Puppi D, Chiellini F, Dash M and E C, Biodegradable Polymers for Biomedical Applications, in *Biodegradable Polymers: Processing, Degradation & Applications*, ed by Felton GP. Nova Science Publishers, New York, pp. 545-560 (2011).
28. Woodruff MA and Hutmacher DW, *Prog Polym Sci* **35:1217-1256**: (2010).
29. Puppi D, Mota C, Gazzarri M, Dinucci D, Gloria A, Myrzabekova M, Ambrosio L and Chiellini F, *Biomed Microdevices* **14**: 1115-1127 (2012).
30. Phipps MC, Clem WC, Grunda JM, Clines GA and Bellis SL, *Biomaterials* **33**: 524-534 (2012).
31. Sun H, Mei L, Song C, Cui X and Wang P, *Biomaterials* **27**: 1735-1740 (2006).
32. Zhu J and Marchant RE, *Expert Rev Med Devices* **8**: 607-626 (2011).
33. Tsao CT, Chang CH, Lin YY, Wu MF, Wang J-L, Han JL and Hsieh KH, *Carbohydr Res* **345**: 1774-1780 (2010).
34. Puppi D, Migone C, Morelli A, Bartoli C, Gazzarri M, Pasini D and Chiellini F, *J Bioact Compat Polym* **DOI: 10.1177/0883911516631355**: (2016).
35. Billiet T, Vandenhaute M, Schelfhout J, Van Vlierberghe S and Dubruel P, *Biomaterials* **33**: 6020-6041 (2012).
36. Mota C, Puppi D, Dinucci D, Gazzarri M and Chiellini F, *J Bioact Compat Polym* **28**: 320-340 (2013).
37. Visser J, Melchels FPW, Jeon JE, van Bussel EM, Kimpton LS, Byrne HM, Dhert WJA, Dalton PD, Hutmacher DW and Malda J, *Nat Commun* **6**: Article number: 6933 (2015).
38. Shin SR, Bae H, Cha JM, Mun JY, Chen Y-C, Tekin H, Shin H, Farshchi S, Dokmeci MR, Tang S and Khademhosseini A, *ACS Nano* **6**: 362-372 (2012).

39. Saez-Martinez V, Garcia-Gallastegui A, Vera C, Olalde B, Madarieta I, Obieta I and Garagorri N, *J Appl Polym Sci* **120**: 124-132 (2011).
40. Maranchi JP, Trexler MM, Guo Q and Elisseeff JH, *Int Mater Rev* **59**: 264-296 (2014).
41. Yodmuang S, McNamara SL, Nover AB, Mandal BB, Agarwal M, Kelly T-AN, Chao P-hG, Hung C, Kaplan DL and Vunjak-Novakovic G, *Acta Biomater* **11**: 27-36 (2015).
42. Moutos FT, Freed LE and Guilak F, *Nat Mater* **6**: 162-167 (2007).
43. Liao IC, Moutos FT, Estes BT, Zhao X and Guilak F, *Adv Funct Mater* **23**: 5833-5839 (2013).
44. Marijnissen WJCM, van Osch GJVM, Aigner J, van der Veen SW, Hollander AP, Verwoerd-Verhoef HL and Verhaar JAN, *Biomaterials* **23**: 1511-1517 (2002).
45. Yu H-S, Won J-E, Jin G-Z and Kim H-W, *BioRes Open Access* **1**: 124-136 (2012).
46. Pati F, Jang J, Ha D-H, Won Kim S, Rhie J-W, Shim J-H, Kim D-H and Cho D-W, *Nat Commun* **5**: Article number: 3935 (2014).
47. Schuurman W, Khristov V, Pot MW, Weeren PRv, Dhert WJA and Malda J, *Biofabrication* **3**: 021001 (2011).
48. Lee H, Ahn S, Bonassar LJ and Kim G, *Macromol Rapid Commun* **34**: 142-149 (2013).
49. Cha C, Soman P, Zhu W, Nikkhah M, Camci-Unal G, Chen S and Khademhosseini A, *Biomater Sci* **2**: 703-709 (2014).
50. Agrawal A, Rahbar N and Calvert PD, *Acta Biomater* **9**: 5313-5318 (2013).
51. Giannitelli SM, Mozetic P, Trombetta M and Rainer A, *Acta Biomaterialia* **24**: 1-11 (2015).
52. Puppi D, Zhang X, Yang L, Chiellini F, Sun X and Chiellini E, *J Biomed Mater Res, Part B* **102**: 1562-1579 (2014).
53. Hoffman AS, *Adv Drug Delivery Rev* **64, Supplement**: 18-23 (2012).
54. Puppi D, Piras AM, Pirosa A, Sandreschi S and Chiellini F, *J Mater Sci: Mater Med* **27**: 44 (2016).
55. Jiang W, Shi J, Li W and Sun K, *J Biomater Sci Polym Ed* **24**: 539-550 (2013).
56. de Britto D and Campana-Filho SP, *Thermochim Acta* **465**: 73-82 (2007).
57. Singh J, Dutta PK, Dutta J, Hunt AJ, Macquarrie DJ and Clark JH, *Carbohydr Polym* **76**: 188-195 (2009).
58. Horn MM, Martins VCA and de Guzzi Plepis AM, *Carbohydr Polym* **77**: 239-243 (2009).
59. Kang H-S, Park S-H, Lee Y-G and Son T-I, *J Appl Polym Sci* **103**: 386-394 (2007).
60. Gloria A, Russo T, De Santis R and Ambrosio L, *J Appl Biomater Biomech* **7**: 141-152 (2009).
61. Coburn J, Gibson M, Bandalini PA, Laird C, Mao H-Q, Moroni L, Seliktar D and Elisseeff J, *Smart Struct Syst* **7**: 213-222 (2011).
62. Tao X, Kyle WB, Mohammad ZA, Dennis D, Weixin Z, James JY and Anthony A, *Biofabrication* **5**: 015001 (2013).
63. Martínez-Camacho AP, Cortez-Rocha MO, Castillo-Ortega MM, Burgos-Hernández A, Ezquerra-Brauer JM and Plascencia-Jatomea M, *Polym Int* **60**: 1663-1669 (2011).
64. Dash M, Chiellini F, Ottenbrite RM and Chiellini E, *Prog Polym Sci* **36**: 981-1014 (2011).
65. Akıncıbay H, Şenel S and Yetkin Ay Z, *J Biomed Mater Res, Part B* **80B**: 290-296 (2007).
66. Mouriño V and Boccaccini AR, *Journal of the Royal Society Interface* **7**: 209-227 (2010).

Table 1: Structural parameters of PCL and PCL/HA scaffolds with different d_{xy}. Data expressed as average ± standard deviation (n=20).

Scaffold	Inter-fiber needle translation (d_{xy}) (mm)	Fiber Diameter (µm)	Pores size^{+} (µm)
$PCL_{0.5}$	0.5	238.4 ± 13.4	256.3 ± 36.4
$PCL/HA_{0.5}$	0.5	241.7 ± 21.5	262.3 ± 59.5
PCL_1	1.0	222.1 ± 11.7	812.5 ± 65.4
PCL/HA_1	1.0	240.7 ± 13.4	807.5 ± 41.8
$PCL_{1.5}$	1.5	231.1 ± 14.6	1292.3 ± 45.2
$PCL/HA_{1.5}$	1.5	245.2 ± 16.1	1257.8 ± 61.2
PCL_2	2.0	258.4 ± 16.1*	1732.1 ± 52.8
PCL/HA_2	2.0	261.7 ± 21.5**	1742.4 ± 53.6

*, ** Parameters significantly different ($p < 0.05$) in comparison to the other scaffolds with the same composition and different d_{xy}.
$^{+}$ Pore size of scaffolds with different d_{xy} are significantly different ($p < 0.05$).

Table 2. Thermal parameters obtained from TGA and DSC analysis. Data expressed as average ± standard deviation (n=3).

Sample	T_{onset} (°C)	Tg (°C)		Tm (°C)		Cristallinity (%)	
		1st heating	2nd heating	1st heating	2nd heating	1st heating	2nd heating
PCL raw	385.76 ± 0.91	-61,82 ± 1,05	-61,66 ± 1,51	59,38 ± 0,68*	58,37 ± 1,08	57,40 ± 2,22*	49,10 ± 2,06
PCL_1	385.47 ± 1.10	-58,26 ± 1,46	-62,69 ± 0,76	65,02 ± 1,19	57,11 ± 0,85	69,76 ± 2,91	50,05 ± 2,27
PCL/HA_1	347.26 ± 11.18*	-58,58 ± 1,12	-62,67 ± 0,37	63,92 ± 0,87	57,89 ± 0,54	70,07 ± 1,88	49,40 ± 1,36
PCL_1-CS/γPGA	378.76 ± 2.29**	-59,99 ±1,71	-62,55 ± 0,43	64,74 ± 0,91	60,12 ±2,50	68,14 ± 5,05	48,31 ± 2,62

, * Value significantly different when compared to those of other scaffold types

Table 3. Mechanical parameters of the investigated scaffolds and a CS/γ-PGA hydrogel. Data expressed as average ± standard deviation (n=5).

Scaffold	E (Mpa)	Stress at 50% strain (Mpa)	Stress at 90% strain (Mpa)
PCL_1	1,3401 ± 0,1923	0,6858 ± 0,0524	2,0599 ± 0,4039
$PCL_{1.5}$	0,2158 ± 0,0350	0,2203 ± 0,0350	0,5208 ± 0,0643
PCL/HA_1	1,2375 ± 0,2282	0,4880 ± 0,2282	1,5886 ± 0,4041
$PCL/HA_{1.5}$	0,2932 ± 0,0250	0,1861 ± 0,0116	0,5368 ± 0,0125
PCL_1-CS/ γ-PGA	0,1472 ± 0,0808	0,2305 ± 0,0155	4,3294 ± 2,5378
$PCL_{1.5}$-CS/γ-PGA	0,0907 ± 0,0614	0,1205 ± 0,0185	1,5299 ± 1,0886
PCL/HA_1-CS/γ-PGA	0,0348 ± 0,0114	0,1657 ± 0,0426	3,2829 ± 2,7545
$PCL/HA_{1.5}$-CS/ γ-PGA	0,0249 ± 0,0046	0,0941 ± 0,0137	5,1500 ± 2,1911
CS/γ-PGA hydrogel	0,0014 ± 0,0005	0,0047 ± 0,0039	0,1930 ± 0,1231